

Targeted gene knockout in mammalian cells by using engineered zinc-finger nucleases

Yolanda Santiago*, Edmond Chan*, Pei-Qi Liu*, Salvatore Orlando*, Lin Zhang†, Fyodor D. Urnov*, Michael C. Holmes*, Dmitry Guschin*, Adam Waite*, Jeffrey C. Miller*, Edward J. Rebar*, Philip D. Gregory**‡, Aaron Klug‡§, and Trevor N. Collingwood*

*Sangamo BioSciences, Inc., 501 Canal Boulevard, Suite A100, Richmond, CA 94804; †Pfizer, Inc., Bioprocess Research and Development, Cell Line Development, 700 Chesterfield Parkway West, Chesterfield, MO 63017; and ‡Medical Research Council Laboratory of Molecular Biology, Hills Road, Cambridge CB2 2QH, United Kingdom

Contributed by Aaron Klug, January 30, 2008 (sent for review November 14, 2007)

Gene knockout is the most powerful tool for determining gene function or permanently modifying the phenotypic characteristics of a cell. Existing methods for gene disruption are limited by their efficiency, time to completion, and/or the potential for confounding off-target effects. Here, we demonstrate a rapid single-step approach to targeted gene knockout in mammalian cells, using engineered zinc-finger nucleases (ZFNs). ZFNs can be designed to target a chosen locus with high specificity. Upon transient expression of these nucleases the target gene is first cleaved by the ZFNs and then repaired by a natural—but imperfect—DNA repair process, nonhomologous end joining. This often results in the generation of mutant (null) alleles. As proof of concept for this approach we designed ZFNs to target the dihydrofolate reductase (DHFR) gene in a Chinese hamster ovary (CHO) cell line. We observed biallelic gene disruption at frequencies >1%, thus obviating the need for selection markers. Three new genetically distinct *DHFR*^{-/-} cell lines were generated. Each new line exhibited growth and functional properties consistent with the specific knockout of the DHFR gene. Importantly, target gene disruption is complete within 2–3 days of transient ZFN delivery, thus enabling the isolation of the resultant *DHFR*^{-/-} cell lines within 1 month. These data demonstrate further the utility of ZFNs for rapid mammalian cell line engineering and establish a new method for gene knockout with application to reverse genetics, functional genomics, drug discovery, and therapeutic recombinant protein production.

genetic engineering | zinc-finger proteins

The use of gene knockouts in basic research, functional genomics, and industrial cell line engineering is severely limited by an absence of methods for rapid targeting and disruption of an investigator-specified gene. Early approaches to somatic cell gene disruption used genome-wide nontargeted methods, including ionizing radiation and chemical-induced mutagenesis (1, 2) whereas more recent methods used targeted homologous recombination (HR) (3). However, the >1,000-fold lower frequency of the targeted HR event relative to random integration in most mammalian cell lines (beyond mouse ES cells) can necessitate screening thousands of clones and take several months to identify a biallelic targeted gene knockout. Strategies including positive and negative marker selection and promoter-trap can boost efficiencies considerably, although these approaches present their own technical challenges and are not always successful in achieving high efficiency targeting (4, 5). Although advances with adeno-associated viral delivery strategies continue to improve the efficiency of knockouts (6, 7), the frequency is still very low and the time required to achieve biallelic gene knockout remains a barrier to its routine adoption. Here, we present a general solution for rapid gene knockout in mammalian cells.

The repair of double strand DNA breaks (DSB) in mammalian cells occurs via the distinct mechanisms of homology directed repair (HDR) or nonhomologous end joining (NHEJ) (8).

Although HDR typically uses the sister chromatid of the damaged DNA as a template from which to perform perfect repair of the genetic lesion, NHEJ is an imperfect repair process that often results in changes to the DNA sequence at the site of the DSB. During NHEJ, the cleaved DNA is further resected by exonuclease activity, and more bases may be added in an irregular fashion before the two ends of the severed DNA are rejoined (9). In mammalian systems, such as Chinese hamster ovary (CHO) cells, the ratio of HDR to NHEJ-based repair has been found to be 9:13 (10). Studies in *Drosophila* (11) and later in both plants and worms (12, 13) showed that DSBs generated by site-specific zinc-finger nucleases (ZFNs) resulted in targeted mutagenesis consistent with repair by NHEJ. In this article, we now extend the ZFN approach to mammalian systems. We make use of the process of NHEJ to carry out targeted gene knockout in CHO cells by using transiently expressed site-specific ZFNs to generate the DSB in the gene that is being targeted (for reviews, see refs. 14 and 15).

ZFNs employ a heterologous zinc-finger protein (ZFP) DNA binding domain (which specifically binds to the designated target sequence) fused to the catalytic domain of the endonuclease FokI (16). Dimerization of this FokI domain is required for its DNA binding-dependent endonuclease activity. Thus, two individual ZFNs are designed as a pair to bind to the target DNA stretch with precise sequence specificity, spacing, and orientation to facilitate dimerization and subsequent DNA cleavage (11, 16). When expressed transiently in cells, the ZFNs generate a site-specific DSB in the endogenous target gene that subsequently can be repaired via NHEJ. The precise nature of the mutations generated by NHEJ-based repair of the ZFN-induced DSB cannot be predetermined and, indeed, need not be known. In this article, we show that the frequency of gene disrupting mutations generated by this stochastic process is more than sufficient for utility as a method for gene knockout.

To demonstrate the ZFN approach to gene knockout, we elected to disrupt the function of the dihydrofolate reductase (DHFR) gene in a Chinese hamster ovary cell line (CHO-S) that is diploid for functional DHFR. CHO cells are the dominant

Author contributions: P.-Q.L., F.D.U., M.C.H., D.G., J.C.M., E.J.R., P.D.G., and T.N.C. designed research; Y.S., E.C., P.-Q.L., S.O., A.W., and J.C.M. performed research; P.-Q.L., L.Z., E.J.R., P.D.G., and T.N.C. analyzed data; and P.D.G., A.K., and T.N.C. wrote the paper.

Conflict of interest statement: Y.S., E.C., P.-Q.L., S.O., F.D.U., M.C.H., D.G., J.C.M., E.J.R., P.D.G., and T.N.C. are full-time employees of Sangamo BioSciences, Inc. A.K. is a member of the scientific advisory board for Sangamo BioSciences, Inc. L.Z. is a full-time employee of Pfizer, Inc.

Freely available online through the PNAS open access option.

See Commentary on page 5653.

†To whom correspondence may be addressed. E-mail: pgregory@sangamo.com or akl@mrc-lmb.cam.ac.uk.

This article contains supporting information online at www.pnas.org/cgi/content/full/0800940105/DCSupplemental.

© 2008 by The National Academy of Sciences of the USA

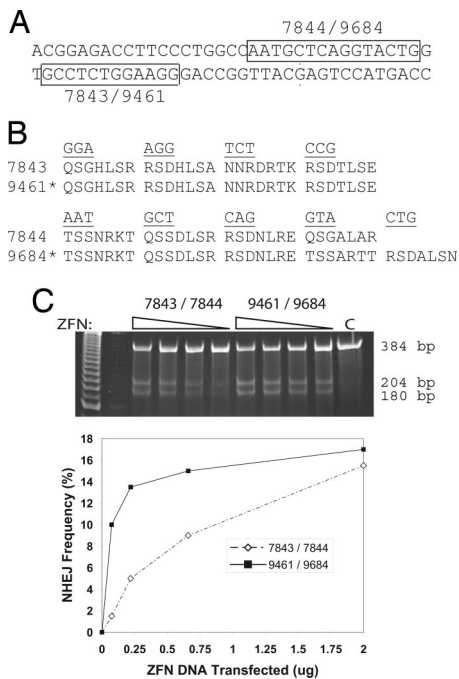


Fig. 1. Targeting the *DHFR* locus with designed ZFNs. (A) Section of the *DHFR* gene targeted by ZFNs. The DNA sequence of the primary binding site for each ZFN is boxed. ZFN7843 and ZFN9461 bind the same 12-bp site. ZFN7844 binds the 12-bp site AATGCTCAGGTA, whereas ZFN9684 binds the 15-bp site AATGCTCAGGTACTG. (B) Recognition helix sequences of ZFNs. The sequence of the recognition helix from position -1 to $+6$ (27) is listed below its target triplet. Backbone sequences for the ZFNs can be found elsewhere (20). The C-terminal finger recognizes the 5' most DNA triplet. The asterisks denote that these ZFNs employ the ELKK variant FokI domains throughout. (C) Comparison of ZFN activity. Plasmids encoding each pair of ZFNs (ZFN7843/ZFN7844 and ZFN9461/ZFN9684) containing the ELKK FokI variants were delivered in the amounts shown to CHO-S cells in suspension culture. The frequency of allelic mutation in each pool of treated cells was determined by using the CEL-I assay (gel). Bands migrating at 384, 204, and 180 bp represent the parent amplicon and the two CEL-I digestion products, respectively. The bands were quantitated by EtBr staining and densitometry to determine the frequency of NHEJ. The frequency of NHEJ is plotted against ZFN dosage. The lowest band on the 25-bp size ladder is 125 bp.

system for the production of therapeutic recombinant proteins (17). *DHFR* is one of the most widely used and best characterized selectable marker genes and is used in conjunction with CHO cell lines in which endogenous *DHFR* expression has been destroyed. This widespread familiarity with *DHFR* makes it an ideal choice of target gene with which to validate a ZFN-mediated approach to gene knockout. Furthermore, existing *DHFR*-negative CHO cell lines provide additional benchmarks against which we can verify the phenotype of our ZFN-generated *DHFR* knockout cell lines. Here, we report (i) the successful generation of ZFNs targeting the *DHFR* locus in CHO-S cells and (ii) the application of these ZFNs to generate stable cell lines devoid of functional *DHFR*.

Results

Design of Zinc Finger Nucleases Targeting the *DHFR* Gene. Exon 1 of the CHO-S *DHFR* locus was chosen for targeting with pairs of ZFNs, using the same strategy as in ref. 16. Structural studies of human *DHFR* have shown this region to be critical for substrate and cofactor binding (18). ZFNs that form pairs, which target the *DHFR* locus, were designed and screened *in vitro* for DNA binding to their target sites (Fig. 1 A and B and data not shown), using an ELISA-based assay (19). The nuclease function of ZFNs is conferred by the catalytic domain of the endonuclease

FokI, which is linked to the DNA-binding zinc-finger proteins. Two different architectures of the FokI catalytic domain were tested, either the WT FokI domain or the high-fidelity FokI-KK and FokI-EL obligate heterodimer (ELKK) variants described in ref. 20. These FokI dimerization variants provide an additional level of specificity to ZFN cleavage by effectively eliminating unwanted homodimerization events elsewhere in the genome (20, 21). The ZFN9461/ZFN9684 pair used the ELKK FokI variants in all cases. The ZFN7843/ZFN7844 pair used the WT FokI domain in all studies except that shown in Fig. 1C. For this experiment, all ZFNs used the ELKK variants so that the only experimental variable was the structure of the DNA binding domains themselves (Fig. 1B). Plasmids expressing each pair of ZFNs were transfected into cells at the reported amount. The frequency of ZFN-mediated disruption at the target site in each pool of cells was determined by using the CEL-I nuclease assay (see *Materials and Methods* for discussion of this assay). We found that expression of the ZFN9461/ZFN9684 pair gave enhanced targeted gene cleavage compared with that shown by the ZFN7843/ZFN7844 pair, as demonstrated by the increased incidence of allelic mutation (NHEJ frequency) in the ZFN-treated pools, particularly at lower levels of input ZFN (Fig. 1C). Although both ZFN pairs attained a similar maximum level of *in vivo* gene cleavage ($\approx 15\%$), the ZFN9461/ZFN9684 pair achieved this by using ≈ 10 -fold less ZFN plasmid. Taken together, these data demonstrate that the ZFN7843/ZFN7844 and ZFN9461/ZFN9684 pairs successfully cleave, and thereby initiate mutation of, the target locus within exon 1 of the CHO-S *DHFR* gene.

Generation of *DHFR*-Deficient Cell Lines. *DHFR*^{-/-} cell lines were generated by transfecting CHO-S cells with either of the ZFN pairs described above and then plating at limiting dilution to obtain single-cell derived *DHFR*-deficient cell lines. This approach was tested in two separate studies. In the first study, CHO-S cells growing adherently in serum-containing medium were treated with the ZFN7843/ZFN7844 pair containing the WT FokI domain. After dilution cloning (one cell per well average), 68 isolates were analyzed for *DHFR* gene disruption, using the CEL-I assay. Five of 68 isolates (7%) showed the presence of mutated *DHFR* alleles and were further subcloned to ensure clonal purity. The exact sequence of the mutant alleles in each cell line, and thus the genotype, was determined by PCR-amplifying the target locus and cloning the PCR product, then sequencing ≈ 90 of the resulting bacterial colonies—each of which contained the sequence of either allele. Three of the clones appeared to be heterozygous for *DHFR* disruption (data not shown). The remaining two clones, 14/1 and 14/2, showed no WT sequence, suggesting biallelic disruption. For clone 14/1, 47 of the 89 sequence reads (53%) showed a single base pair insertion between the ZFN binding sites, whereas the remaining 42 reads (47%) indicated a 2-bp insertion in the same region (Fig. 2A). The $\approx 1:1$ ratio of alleles indicated that clone 14/1 is a compound heterozygous mutant in which both alleles have mutations between the individual ZFN binding sites that result in shifts in reading frame. These give rise to premature termination products of 46 and 38 codons, respectively, and the mutant mRNA transcripts are also expected to undergo nonsense-mediated decay. Clone 14/2 is also a compound heterozygous mutant from which 43 sequence reads contained the same 2-bp insertion present in clone 14/1, but the remaining 40 contained a 15-bp deletion (Fig. 2A). Although the deletion preserves the reading frame for the *DHFR* protein, the five amino acid residues (ProTrpProMetLeu) deleted from this peptide are critical to the integrity of the ligand-binding pocket of *DHFR* (18).

In the second study, CHO-S cells cultured in serum-free suspension medium were transfected with the other ZFN pair,

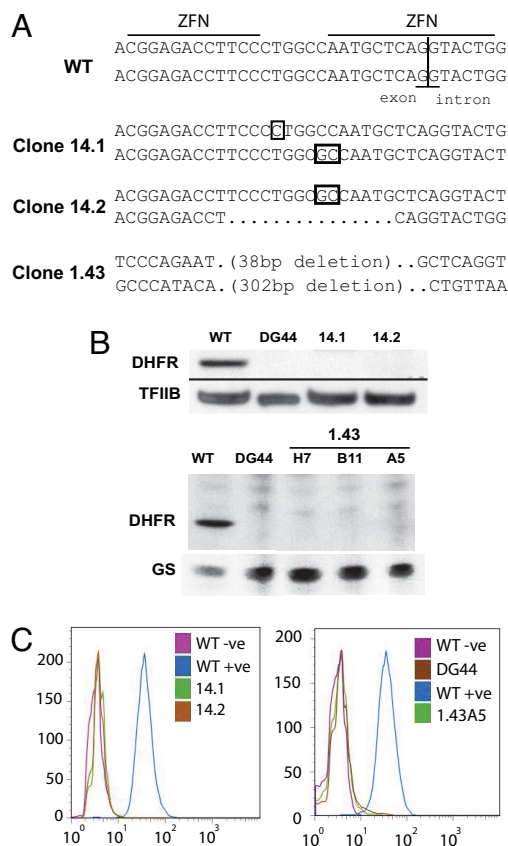


Fig. 2. Genotype and phenotype of ZFN-induced *DHFR*^{-/-} clones from CHO-S cells. (A) Each pair of sequences represents the two alleles of the *DHFR* gene in the designated cell line. For each mutant allele, inserted bases are boxed, and deleted bases are represented by dots. (B) Western blot for DHFR protein in WT CHO-S cells (WT) and the mutant cell lines 14/1, 14/2, and 1.43 and the commercially available DHFR-null CHO cell line DG44. Note that, for clone 1.43, we analyzed three independent subclones from this line (H7, B11, and A5). Input is normalized against TFIIB or glutamine synthetase (GS) expression levels as indicated. (C) Fluorescein-labeled methotrexate (FMTX)-based FACS analysis of *DHFR*^{-/-} cell lines. WT(-ve), WT CHO-S cells not treated with FMTX; WT(+ve), WT CHO-S cells treated with FMTX. All mutant cell lines were treated with FMTX, including DG44 as a DHFR-null CHO cell control. (Left) Cells in adherent culture. (Right) Cells in suspension culture.

ZFN9461/ZFN9684, but, in this case, the ELKK FokI variant domains were used. After dilution cloning, 350 isolates were analyzed via direct sequencing of PCR products of the genomic target locus. Eleven of these clones (3%) were found to have at least one disrupted copy of the *DHFR* gene (data not shown). Upon further cloning and sequencing of these PCR products (as in the first study), four were found to be compound heterozygous for mutations in both copies of the *DHFR* gene, with the remaining seven clones being heterozygous. All mutations were centered on the ZFN cleavage site, and all were consistent with functional *DHFR* disruption—either by deletion of critical residues or by introduction of a frameshift. Most mutations we observed were small deletions (<20 bp). Clone 1.43 (and the subclone 1.43A5; data not shown) exhibited the largest genetic loss of all clones analyzed, with a 302-bp deletion in one allele and a 38-bp deletion in the other allele (Fig. 2A). Both mutations extended into the following intron, eliminating a splice site, and thus would be expected to result in the loss of functional *DHFR* expression.

For each of the three *DHFR*^{-/-} cell lines produced in the above two studies, no DHFR protein could be detected by Western blot analysis using an antibody that recognizes the

carboxyterminal region of DHFR (Fig. 2B). Although the mutant allele that encodes a 5-aa deletion in clone 14/2 might have been expected to generate a near-full length, albeit nonfunctional, peptide, the Western blot analysis indicates that this peptide is unstable, perhaps eliminated via the unfolded protein response (22). To further confirm the loss of functional DHFR, we used a fluorescence-based assay to detect the binding of fluorescein-labeled methotrexate (FMTX), which would indicate the presence of functional endogenous DHFR (23). We observed that all three *DHFR*^{-/-} lines did not bind FMTX, in contrast to the WT parental CHO-S cells (Fig. 2C). This result further confirms the loss of functional DHFR protein expression in all three genetically distinct *DHFR*^{-/-} cell lines generated from this study.

Functional Analysis of DHFR Knockout Cell Lines. DHFR catalyzes the reduction of folate during the biosynthesis of purines, thymidine, and glycine. DHFR negative cells are unable to grow unless the culture medium is supplemented with essential metabolites, including hypoxanthine and thymidine (HT) (1). To confirm the loss of functional DHFR expression, each *DHFR*^{-/-} cell line was cultured for 4 days in medium either with or without HT supplement. As predicted, *DHFR*^{-/-} cell lines 14/1 and 14/2 (Fig. 3A Upper) and 1.43A5 (Fig. 3A Lower) exhibited a strict requirement for HT. DHFR is frequently used as a selection marker for the stable expression of recombinant proteins in DHFR-deficient mammalian cell lines. To further validate the new cell lines described above, we investigated their capacity to support DHFR-based selection of transgene expression. Each mutant cell line and WT CHO-S cells were transfected with plasmids driving coexpression of a monoclonal antibody and a DHFR gene as the selection marker. All cells produced similar levels of antibody two days after transient transfection of the expression constructs (data not shown). However, after 2 weeks of culture in the absence of HT supplement, we observed that stable pools derived from each *DHFR*^{-/-} clone exhibited significantly greater antibody expression levels than did those derived from WT cells (Fig. 3B). This result is consistent with the need for these *DHFR*^{-/-} cells to retain coselected exogenous DHFR expression for survival in the absence of HT, whereas the WT cells were under no such selection pressure. Conversely, the *DHFR*^{-/-} cell lines did not exhibit increased antibody expression when selection pressure was not applied (i.e., when HT was present). Furthermore, subsequent incubation of the “minus-HT-selected” antibody-expressing pool from cell line 14/1 in the presence of 50 nM or 250 nM the DHFR inhibitor methotrexate resulted in an increase in antibody expression of 1.7-fold and 2.6-fold, respectively (Fig. 3C). This reflects the selection of cells that exhibit higher levels of DHFR expression and therefore elevated levels of coselected antibody. Increased antibody expression in the pools is likely due to amplification of gene copy number (24) and/or selection of clones in which the transgenes have randomly integrated into chromosomal loci that are more permissive for gene expression. Taken together, the results obtained in these DHFR selection and amplification studies are consistent with the characterized behavior of other DHFR-negative CHO cells (24) and thus further support the phenotype of the cell lines described here.

It may be relevant to add that, except for the loss of endogenous DHFR expression, the cells we have isolated behave in all other respects like WT CHO-S. For example, clone 1.43A5 exhibits a doubling time of 16.8 h, which is comparable with that of WT (14.1 h; data not shown), and chromosomal integrity is also generally preserved [supporting information (SI) Fig. S1]. These observations further support the notion that ZFN-mediated gene targeting can be performed without significant unwanted genetic or phenotypic disruption.

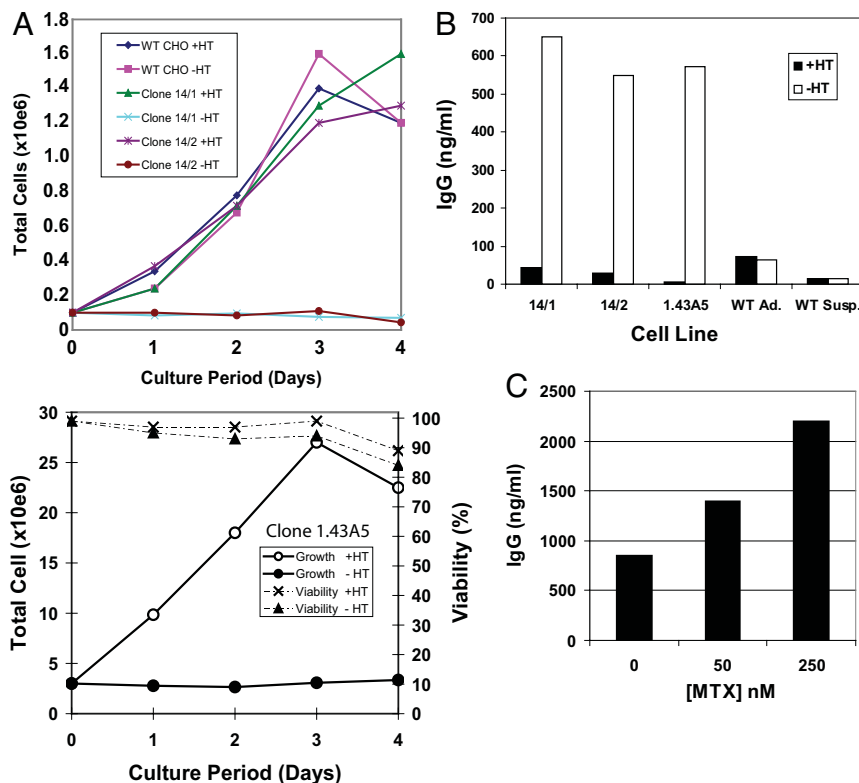


Fig. 3. Growth and functional properties of the ZFN-generated *DHFR*^{-/-} cell lines. (A) WT CHO-S (WT CHO) and ZFN-generated *DHFR*^{-/-} CHO-S cell lines were cultured in the presence or absence of HT supplement as indicated. (Upper) Growth of *DHFR*^{-/-} cell lines 14/1 and 14/2 compared with WT CHO cells in adherent culture conditions. (Lower) Growth and viability of the *DHFR*^{-/-} cell line 1.43A5 in serum-free suspension culture. (B) IgG expression from WT or *DHFR*^{-/-} cell lines after transfection with antibody expression constructs coexpressing a DHFR gene as a selection marker. Cells were cultured in the presence (+HT) or absence (-HT) of HT supplement for 14 days. IgG expression at >48 h was measured by ELISA. WT Ad., WT CHO-S cells in adherent medium; WT Susp., WT CHO-S cells in suspension medium. Cell lines 14/1 and 14/2 were cultured adherently. Cell line 1.43A5 was cultured in suspension. (C) Methotrexate selection/amplification in *DHFR*^{-/-} cell line 14/1. Data shown is the level of IgG stably expressed from a clone 14/1 pool after 2 weeks of incubation in the absence of HT then 2 weeks more in the presence of the noted concentration of methotrexate (see *Materials and Methods*).

Discussion

This study demonstrates the feasibility of a ZFN-based approach to rapid targeted gene knockout in cultured cells. The targeted gene mutation frequency was sufficient to identify biallelic knockouts after a single transient ZFN treatment and without the need for selection methodologies. In the present study, the frequency of mutated alleles detected upon screening of clones (2–3%) was lower than expected given the initial level of NHEJ measured in the treated pool (15%; Fig. 1C). This may be due to a selective growth disadvantage of clones that are deficient in endogenous DHFR expression despite the presence of HT in the medium. Nevertheless, >1% of all clones analyzed showed biallelic modification. We have reported that the targeting of each of the two copies of a gene within a given single cell does not appear to be an independent event (16). Our observation here that approximately one-third of all mutant clones have biallelic modification is consistent with this. Taken together, these data demonstrate that the reduced screening effort needed to identify a ZFN-mediated biallelic disruption at a specific locus—in the absence of selection—offers a significant advantage compared with existing methods.

In previous reports, we have demonstrated that ZFNs are powerful tools for gene modification by harnessing homologous recombination from an extrachromosomal donor (16, 25). Here, we have omitted the donor DNA, relying instead simply on NHEJ-derived modifications, which are effectively random, leading to a mutated gene with knocked out function. Our method also contrasts with the original demonstration of mutating or knocking out

a gene where “gene targeting” was driven only by the homology with the DNA donor (3). The NHEJ method we describe is a simple and rapid method for gene knockout.

Abrogating the need for a homologous donor thus simplifies the approach to ZFN-mediated high-efficiency gene knockout and eliminates the use of selection markers that may hamper the utility of the cell line for certain industrial applications (see below). Rather, the simplicity of the process described here is driven by the naturally random nature of this mode of repair that frequently results in a gain or loss of genetic information at the target locus sufficient to disrupt gene expression. As we have seen, this can occur by causing a shift in reading frame to generate a premature termination codon (and possibly destruction of the mRNA by nonsense-mediated decay), as for cell lines 14/1 and 1.43A5, or by deletion of critical amino acid residues, as with cell line 14/2. NHEJ-based DNA repair is inherently less precise in that a specific genetic outcome is not predetermined by donor DNA design, but this is not relevant to our purpose here. The high frequencies of gene disruption strongly support the likelihood of readily achieving the desired genotype in which each copy of the target gene is functionally knocked out.

In the absence of viable methods for rapid gene knockout, several new technologies (e.g., antisense, RNAi, and zinc finger protein transcription factors) have been developed recently that enable the knockdown of gene expression, sometimes achieving >90% reduction in target gene levels for as long as the repressor molecules are present (26). The ease and

rapidity of use of some of these approaches has made them the method of choice for applications such as initial target validation. However, possible toxicity effects on their long term expression and the incomplete phenotypic penetrance that may arise from partial knockdown of the target gene may prove undesirable. Additional metabolic load on cells due to overexpression of these factors during times of stress (e.g., during large scale fermentation) may also be a concern. In such instances, rapid and permanent gene knockout, using ZFNs, can offer distinct advantages. Moreover, the growing number of reports, using ZFNs across different species (11–13, 16), suggest that ZFN-mediated gene disruption may be a robust and general method for targeted gene knockout.

There are several other critical differences between the present approach and existing methods that offer further advantages. ZFN-mediated gene knockout requires only transient expression of the ZFNs yet results in a permanent genetic mark. Because this is an alteration to the genome itself, the mutation is stably transmitted through all subsequent generations of the cell line, as is the case with conventional gene targeting. Another unique aspect of the ZFN approach is that no selectable markers are required to identify or isolate the targeted events. This has practical value—especially in industrial applications such as recombinant protein manufacture—where the sustained expression of exogenous marker genes is undesirable. It allows also for multiple genes to be targeted without constraints arising from a limited number of available selectable marker genes. This latter point, in conjunction with the speed by which the knockout of any given gene can be achieved, opens up possibilities for multigene targeting, or trait stacking, in ways that have not previously been feasible. Future studies will be aimed at testing this concept.

Materials and Methods

Cell Culture and Transfection. ZFN-mediated DHFR gene knockout was performed in CHO-5 cells (Invitrogen; catalog no. 11619-012), which are functionally diploid for DHFR. As a DHFR-negative control cell line, we used the CHO cell derivative DG44 (Invitrogen, catalog no. 12609-012) in which the DHFR gene had been completely disrupted by chemical mutagenesis and ionizing radiation (2). For adherent culture, WT CHO-5 cells clones and all derivative mutant cell lines were grown in DMEM (Invitrogen; catalog no. 11965-092), supplemented with 10% FBS (JRH BioSciences; catalog no. 12117-500M), 10 mM NonEssential Amino Acids (Invitrogen; catalog no. 11140-050), 8 mM L-Glutamine (Invitrogen; catalog no. 25030-081), and 1 × HT supplement (100 μM sodium hypoxanthine and 16 μM thymidine; Invitrogen; catalog no. 11067-030) where specified. For ZFN transfections, the cells were seeded at 3 × 10⁵ cells per well in 24-well dishes. The next day, cells were transfected with 100 ng of each ZFN expression plasmid (in pairs) + 400 ng of pCDNA, using Lipofectamine2000. After 72 h, cells were replated in 96-well format at limiting dilution (1 cell per well on average). CHO DG44 cells were cultured as per the manufacturers recommended protocol.

Suspension cultured CHO-5 cells and all derivative clones were grown and maintained as 30-ml suspension cultures in EX-CELL CD CHO serum-free medium (Sigma-Aldrich; catalog no. 14361C) supplemented with 8 mM L-glutamine in a humidity-controlled shaker incubator (ATR, Inc.) at 125 rpm with 5% CO₂ at 37°C. For studies showing the dependence of the DHFR knockout cell lines on supplemental HT, we used similar medium that was deficient in HT (Sigma-Aldrich; catalog no. 14360C) but also contained 8 mM added glutamine. Cells were transfected with up to 2 μg of each ZFN plasmid, using Amaxa Nucleofector II according to manufacturer's protocol. Viability was measured by trypan blue staining.

CEL-I Nuclease Mismatch Assay. The frequency of targeted gene mutation in ZFN-treated pools of cells was determined by using the CEL-1 nuclease assay as described in ref. 20. This assay detects alleles of the target locus that deviate from WT as a result of NHEJ-mediated imperfect repair of ZFN-induced DNA double strand breaks. PCR amplification of the targeted region from a pool of ZFN-treated cells generates a mixture of WT and mutant amplicons. Melting and reannealing of this mixture results in mismatches forming between heteroduplexes of the WT and mutant alleles. A DNA “bubble” formed at the site of mismatch is cleaved by the surveyor nuclease CEL-1, and the cleavage products can be resolved by gel electrophoresis and quantitated by densitometry. The relative intensity of the cleavage products compared with the parental band is a measure of the level of CEL-1 cleavage of the heteroduplex. This, in turn, reflects the frequency of ZFN-mediated cleavage of the endogenous target locus that has subsequently undergone imperfect repair by NHEJ. The sequence of PCR primers used for amplification of the DHFR target locus is: Forward primer (129F), 5'-TAGGATGCTAGGCTTGTGAGG; Reverse primer (130R), 5'-GCAAAGCTGGCACAGCATG. A 384-bp PCR product was generated from WT genomic sequence.

Western Blot Analysis. The primary antibody used to detect DHFR was from Santa Cruz Biotechnology (catalog no. sc-14780); for detection of TFIIB, the antibody was from Santa Cruz Biotechnology (catalog no. scsc-225); and, for glutamine synthetase, the antibody was from BD Bioscience (catalog no. 610517).

Fluorescent Methotrexate (FMTX) Assay. HT-supplemented growth medium was used throughout. The medium on 1 × 10⁶ cells was replaced with 500 μl of fresh medium containing 10 μM FMTX (Invitrogen; catalog no. M1198MP) and incubated at 37°C for 2 h. The medium was then replaced with 1 ml of fresh medium without FMTX and incubated 30 min at 37°C. Cells were washed once with PBS and resuspended in PBS + 1% FBS at a density of 1 × 10⁵ cells per ml. 5,000 cells per sample were assessed by using a fluorescent cell analyzer (Guava EasyCyte; Guava Technologies) with excitation at 496 nm and emission at 516 nm.

Antibody Expression and ELISA. WT and *DHFR*^{-/-} cells were grown initially in medium supplemented with HT. Cells (1 × 10⁶) were cotransfected with 2 μg of each of two monoclonal antibody expression plasmids in which one contained an expression cassette for the antibody light chain, whereas the other contained a cassette for the antibody heavy chain and a cassette for DHFR expression. The following day, the growth medium was replaced with or without HT supplement, and the cells were left to grow for up to 14 days, changing the medium at 3- or 4-day intervals. After 14 days, 1 × 10⁶ cells were inoculated into 1.0 ml of fresh HT-supplemented medium. After 48 h, the medium was collected and analyzed for antibody expression by ELISA according to manufacturers protocol (Bethyl Laboratories; Human IgG ELISA quantitation kit, catalog no. E80-104).

Methotrexate Selection. The *DHFR*^{-/-} cell line 14/1 was transfected with the antibody constructs described above and grown adherently in the absence of HT supplement for 2 weeks. Methotrexate was then added to the medium at the noted concentration followed by a further 2 weeks of incubation. The growth medium was then removed, and 1.0 ml of fresh HT-supplemented medium was added. After 48 h, the medium from each sample was collected and analyzed for antibody expression by ELISA as above.

ACKNOWLEDGMENTS. We thank Yingying Wu, George Katibah, Anna Vincent, and Sarah Hinkley for generation of the ZFN reagents; Jingwei Yu for performing the cytogenetic analyses; and Andreas Reik for helpful discussion and review of the manuscript. Cytogenetic studies were performed in the laboratory of Dr. Jingwei Yu (Cytogenetics Laboratory, University of California, San Francisco, CA). Early studies leading to this work were supported by Advanced Technology Program grants from the National Institutes of Standards and Technology Grant 70NANB4H3006.

1. Urlaub G, Chasin LA (1980) Isolation of Chinese hamster cell mutants deficient in dihydrofolate reductase activity. *Proc Natl Acad Sci USA* 77:4216–4220.
2. Urlaub G, Kas E, Carothers AM, Chasin LA (1983) Deletion of the diploid dihydrofolate reductase locus from cultured mammalian cells. *Cell* 33:405–412.
3. Mansour SL, Thomas KR, Capecchi MR (1988) Disruption of the proto-oncogene int-2 in mouse embryo-derived stem cells: A general strategy for targeting mutations to non-selectable genes. *Nature* 336:348–352.
4. Vasquez KM, Marburger K, Intody Z, Wilson JH (2001) Manipulating the mammalian genome by homologous recombination. *Proc Natl Acad Sci USA* 98:8403–8410.

5. Yamane-Ohnuki N, et al. (2004) Establishment of FUT8 knockout Chinese hamster ovary cells: An ideal host cell line for producing completely defucosylated antibodies with enhanced antibody-dependent cellular cytotoxicity. *Biotechnol Bioeng* 87: 614–622.
6. Kohli M, Rago C, Lengauer C, Kinzler KW, Vogelstein B (2004) Facile methods for generating human somatic cell gene knockouts using recombinant adeno-associated viruses. *Nucleic Acids Res* 32:e3.
7. Hirata R, Chamberlain J, Dong R, Russell DW (2002) Targeted transgene insertion into human chromosomes by adeno-associated virus vectors. *Nat Biotechnol* 20:735–738.

8. Sonoda E, Hohegger H, Saberi A, Taniguchi Y, Takeda S (2006) Differential usage of non-homologous end-joining and homologous recombination in double strand break repair. *DNA Repair (Amst)* 5:1021–1029.
9. Weterings E, van Gent DC (2004) The mechanism of non-homologous end-joining: A synopsis of synapsis. *DNA Repair (Amst)* 3:1425–1435.
10. Liang F, Han M, Romanienko PJ, Jasin M (1998) Homology-directed repair is a major double-strand break repair pathway in mammalian cells. *Proc Natl Acad Sci USA* 95:5172–5177.
11. Bibikova M, Golic M, Golic KG, Carroll D (2002) Targeted chromosomal cleavage and mutagenesis in *Drosophila* using zinc-finger nucleases. *Genetics* 161:1169–1175.
12. Lloyd A, Plaisier CL, Carroll D, Drews GN (2005) Targeted mutagenesis using zinc-finger nucleases in *Arabidopsis*. *Proc Natl Acad Sci USA* 102:2232–2237.
13. Morton J, Davis MW, Jorgensen EM, Carroll D (2006) Induction and repair of zinc-finger nuclease-targeted double-strand breaks in *Caenorhabditis elegans* somatic cells. *Proc Natl Acad Sci USA* 103:16370–16375.
14. Porteus MH, Carroll D (2005) Gene targeting using zinc finger nucleases. *Nat Biotechnol* 23:967–973.
15. Durai S, et al. (2005) Zinc finger nucleases: Custom-designed molecular scissors for genome engineering of plant and mammalian cells. *Nucleic Acids Res* 33:5978–5990.
16. Urnov FD, et al. (2005) Highly efficient endogenous human gene correction using designed zinc-finger nucleases. *Nature* 435:646–651.
17. Wurm FM (2004) Production of recombinant protein therapeutics in cultivated mammalian cells. *Nat Biotechnol* 22:1393–1398.
18. Klön AE, et al. (2002) Atomic structures of human dihydrofolate reductase complexed with NADPH and two lipophilic antifolates at 1.09 Å and 1.05 Å resolution. *J Mol Biol* 320:677–693.
19. Bartsevich VV, Miller JC, Case CC, Pabo CO (2003) Engineered zinc finger proteins for controlling stem cell fate. *Stem Cell* 21:632–637.
20. Miller JC, et al. (2007) An improved zinc-finger nuclease architecture for highly specific genome editing. *Nat Biotechnol* 25:778–785.
21. Szczepek M, et al. (2007) Structure-based redesign of the dimerization interface reduces the toxicity of zinc-finger nucleases. *Nat Biotechnol* 25:786–793.
22. Zhang K, Kaufman RJ (2006) Protein folding in the endoplasmic reticulum and the unfolded protein response. *Handb Exp Pharmacol* 172:69–91.
23. Gaudray P, Trotter J, Wahl GM (1986) Fluorescent methotrexate labeling and flow cytometric analysis of cells containing low levels of dihydrofolate reductase. *J Biol Chem* 261:6285–6292.
24. Omasa T (2002) Gene amplification and its application in cell and tissue engineering. *J Biosci Bioeng* 94:600–605.
25. Moehle EA, et al. (2007) Targeted gene addition into a specified location in the human genome using designed zinc-finger nucleases. *Proc Natl Acad Sci USA* 104:3055–3060.
26. Tan S, et al. (2003) Zinc-finger protein-targeted gene regulation: Genomewide single-gene specificity. *Proc Natl Acad Sci USA* 100:11997–12002.
27. Pabo CO, Peisach E, Grant RA (2001) Design and selection of novel Cys2His2 zinc finger proteins. *Annu Rev Biochem* 70:313–340.